

Variations in surface water-ground water interactions along a headwater mountain stream: Comparisons between transient storage and water balance analyses

Adam S. Ward,¹ Robert A. Payn,² Michael N. Gooseff,³ Brian L. McGlynn,⁴ Kenneth E. Bencala,⁵ Christa A. Kelleher,³ Steven M. Wondzell,⁶ and Thorsten Wagener^{3,7}

Received 14 June 2012; revised 11 February 2013; accepted 12 February 2013; published 14 June 2013.

[1] The accumulation of discharge along a stream valley is frequently assumed to be the primary control on solute transport processes. Relationships of both increasing and decreasing transient storage, and decreased gross losses of stream water have been reported with increasing discharge; however, we have yet to validate these relationships with extensive field study. We conducted transient storage and mass recovery analyses of artificial tracer studies completed for 28 contiguous 100 m reaches along a stream valley, repeated under four base-flow conditions. We calculated net and gross gains and losses, temporal moments of tracer breakthrough curves, and best fit transient storage model parameters (with uncertainty estimates) for 106 individual tracer injections. Results supported predictions that gross loss of channel water would decrease with increased discharge. However, results showed no clear relationship between discharge and transient storage, and further analysis of solute tracer methods demonstrated that the lack of this relation may be explained by uncertainty and equifinality in the transient storage model framework. Furthermore, comparison of water balance and transient storage approaches reveals complications in clear interpretation of either method due to changes in advective transport time, which sets a the temporal boundary separating transient storage and channel water balance. We have little ability to parse this limitation of solute tracer methods from the physical processes we seek to study. We suggest the combined analysis of both transient storage and channel water balance more completely characterizes transport of solutes in stream networks than can be inferred from either method alone.

Citation: Ward, A. S., R. A. Payn, M. N. Gooseff, B. L. McGlynn, K. E. Bencala, C. A. Kelleher, S. M. Wondzell, and T. Wagener (2013), Variations in surface water-ground water interactions along a headwater mountain stream: Comparisons between transient storage and water balance analyses, *Water Resour. Res.*, 49, 3359–3374, doi:10.1002/wrcr.20148.

1. Introduction

[2] The fluvial processes that drive stream-subsurface exchange are well understood, but our ability to understand their aggregated influence across entire stream networks responding to changing discharge is not as well developed.

Fluxes across the streambed vary at fine spatial scales. As such, these fluxes cannot be directly quantified. Instead, it is common practice to use a limited set of measurements collected at larger spatial scales (e.g., solute tracer studies; *Stream Solute Workshop* [1990]) to summarize surface-subsurface exchange fluxes. Field studies tend to focus on the practical objective of measuring the aggregated effects of surface-subsurface exchange at the spatial scale of hundreds of meters in a stream reach. Examples include using solute tracers to measure the net change in discharge over the reach (identifying gaining or losing stream segments), or to quantify its gross gain and loss components over a stream reach [Payn *et al.*, 2009]. Here we refer to those fluxes as “long-term storage” pathways. We also quantify short-term storage pathways by transient storage modeling of in-stream tracer data. These analyses of long- and short-timescale storage approaches have been widely used though are rarely combined in a single study, especially in an examination of multiple stream reaches throughout a watershed. Changes in both short- and long-term storage with discharge have been reported in the literature. Wondzell [2011, 2012] reported increasing short-term storage with discharge, though the opposite relationship has also

¹Department of Geoscience, The University of Iowa, Iowa City, Iowa, USA.

²Department of Land Resources & Environmental Sciences, Montana State University, Bozeman, Montana, USA.

³Department of Civil and Environmental Engineering, The Pennsylvania State University, University Park, Pennsylvania, USA.

⁴Division of Earth and Ocean Sciences, Nicholas School of the Environment, Duke University, Durham, North Carolina, USA.

⁵U.S. Geological Survey, Menlo Park, California, USA.

⁶U.S. Forest Service, Pacific Northwest Research Station, Corvallis Forestry Sciences Lab, Corvallis, Oregon, USA.

⁷Department of Civil Engineering, University of Bristol, Bristol, UK.

Corresponding author: A. S. Ward, Department of Geoscience, The University of Iowa, 36 Trowbridge Hall, Iowa City, IA 52242, USA. (adam-ward@uiowa.edu)

been reported [e.g., *Jin and Ward, 2005*]. *Covino et al.* [2011] report long-term storage decreasing with increasing discharge. The objective of this study is to determine if stream discharge is a primary factor in establishing short- and long-term storage of solutes and water along the longitudinal axis of a mountain headwater valley. Specifically, we will address three questions: (1) Do metrics of short- and long-term storage follow a consistent spatial pattern with changes in discharge along the longitudinal axis of the stream?, (2) Do metrics of short- and long-term storage follow a consistent temporal pattern with changes in discharge for individual reaches (i.e., through seasonal base-flow recession)?, and (3) Does spatial organization of short- and long-term storage vary across a range of base-flow conditions?

[3] Many stream processes are thought to be organized by position along the stream network (i.e., predictable changes moving downstream along the network). These processes include ecosystem function as described by the river continuum [e.g., *Vannote et al., 1980*]; power law scaling of channel water velocity and cross-sectional geometry [e.g., *Leopold and Maddock, 1953*]; hydrologic dispersion mechanisms [e.g., *Fischer et al., 1979*]; and stream-subsurface exchange as described by the hyporheic corridor [e.g., *Gooseff et al., 2008*; *Stanford and Ward, 1993*]. Synoptic studies at different locations in stream networks rely on the assumption that sparse observations along a network can be used to characterize the gradient in physical processes [e.g., *Briggs et al., 2010*; *Covino et al., 2011*]. Although gradients in physical processes (e.g., transient storage) are expected given the gradients in the physical system [*Schmid et al., 2010*], no study has demonstrated that these gradients exist in short- and long-term storage along contiguous reaches.

[4] In addition to spatial patterns in discharge, predictable changes in solute transport are expected with changing hydrological conditions in a reach (e.g., through base-flow recession). Several studies have used the transient storage model to characterize relationships with discharge by conducting replicate studies in a single reach under different discharges [*Jin and Ward, 2005*]. In these studies, stream discharge had a range of positive, negative, and neutral effects on the extent of transient storage area relative to the extent of the channel area (commonly “storage area ratio,” or “ A_s/A ”) [*Butturini and Sabater, 1999*; *Fabian et al., 2011*; *Hart et al., 1999*; *Karwan and Saiers, 2009*; *Morrice et al., 1997*; *Schmid et al., 2010*; *Wondzell, 2006*; *Zarnetske et al., 2007*]. *Schmid* [2008] demonstrated the applicability of transient storage model parameters across a small range of in-stream discharges for individual reaches. Recent syntheses of tracer studies by *Wondzell* [2011, 2012] suggest short-term storage increases with discharge. While some of these studies include several injections, these data have not been sufficient to characterize solute transport behavior across a wide range of discharges. Too few tracer studies have been analyzed for gross gains and losses to understand how gross changes vary across a wide range of discharges. To address these limitations, we completed transient storage and channel water balance analyses of a series of solute tracer studies. Injections were completed on contiguous 100 m reaches along a 2.8 km valley, under four different base-flow conditions. Using contiguous

reaches and replication of methods under multiple hydrologic conditions allows us to quantify spatial and temporal patterns of short- and long-term storage.

[5] All stream solute tracer studies have an inherent experimental “window of detection” that determines which transient storage flow paths can measurably influence tracer concentrations in the channel water. The duration of this window is strongly influenced by velocity through the channel and discharge. The window of detection describes the temporal suite of flow paths that affect the observed downstream tracer breakthrough curve, typically limiting analysis of recovered tracer to only the most rapid exchanges [for a more complete discussion, see *Harvey et al., 1996*; *Wagner and Harvey, 1997*; *Harvey and Wagner, 2000*]. Thus, we describe these flow paths as “short-term storage” for the purposes of this study. Although the window of detection limits the temporal suite of flow paths characterized as short-term storage, these flow paths exist upon a template that is set by processes occurring at longer temporal and larger spatial scales (for example, patterns of gaining and losing [e.g., *Payn et al., 2009*; *Covino et al., 2011*; *Wondzell and Gooseff, 2011*]). We define the suite of flow paths that do not return to the downstream end of a stream reach within the window of detection of a channel-based tracer experiment as “long-term storage”. Storage in these flow paths may be only incrementally longer than short-term flow paths, or may be as long as regional aquifer storage times. Long-term storage may also represent water that flows in the subsurface to downstream reaches, to deep aquifers, or to riparian evapotranspiration. Regardless of the specific time scale associated with its fate (all flow paths milliseconds beyond the window of detection and longer), this long-term storage manifests as gross gains and losses of channel flow over a given stream reach, where gross gain and loss sum to the net change in discharge. It is also important to note that our measurement of long-term storage will also be influenced by observation time—analogue to the “window-of-detection” for transient storage modeling. Simply put, the amount of time that the tracer mass takes to move the length of the stream reach determines how long tracer-labeled water is exposed to head gradients that drive flux from the channel into the subsurface. Thus, gross fluxes to and from the channel should be inversely related to the velocity and discharge.

[6] The fate of solute beyond the well-mixed, advection-dominated channel could be along flow paths of a wide range of spatial and temporal scales [e.g., *Payn et al., 2009*, Figure 2]. Interpretation of both short- and long-term storage from tracer studies could enhance our understanding of the stream valley hydrologic system beyond interpretation of either short- or long-term storage process alone. We found that the window of detection for solute tracer studies was a primary control on the interpreted short- and long-term storage, limiting our ability to differentiate between unique characteristics of the physical system and its interaction with the methodology applied. Overall, this study relates both short- and long-term storage to existing conceptual frameworks of hyporheic exchange and riparian hydrology, and serves as a direct demonstration of how the “window of detection” complicates the interpretation and scaling of measurements of stream-subsurface exchange.

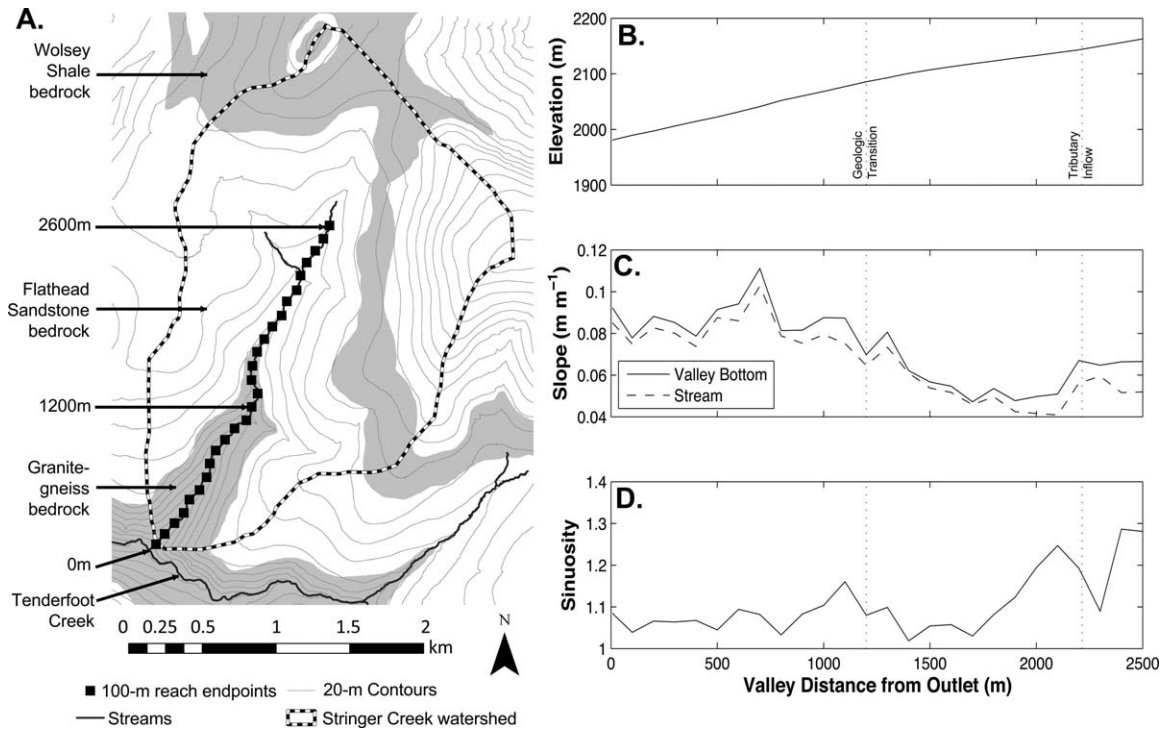


Figure 1. Physical attributes of the Stringer Creek catchment within the Tenderfoot Creek Experimental Forest, Montana, USA. (A) Underlying geology and watershed elevations (reprinted after *Payn et al.* [2009] and *Pail et al.*). (B) Valley bottom elevation along the study reach. (C) Valley bottom and streambed slope. (D) Stream sinuosity.

2. Methods

2.1. Field Site

[7] Field experiments were conducted in the Stringer Creek catchment, a second-order catchment within the Tenderfoot Creek Experimental Forest (Figure 1). The catchment drains a 5.5 km² watershed, and includes ca. 2.6 km of stream valley above the confluence with the Tenderfoot Creek. An unnamed tributary enters the stream 2.2 km upstream of the confluence. There is a transition in valley structure ca. 1.2 km upstream of the confluence with Tenderfoot Creek, apparently corresponding to a transition in underlying bedrock from granite-gneiss (downstream) to sandstone (upstream) [*Reynolds*, 1995]. This transition corresponds to a transition in slope (steeper downstream, flatter upstream) and sinuosity (lower downstream, larger upstream). The upstream valley has a wide floor and shallow slope (5.7%) relative to the downstream valley's narrow riparian zone and steep slope (9.0%) [*Payn et al.*, 2012]. Soil depths in the riparian zone are relatively constant at 1.0–2.0 m deep [*Jencso et al.*, 2009]. No notable changes in the stream morphology were observed during the study.

2.2. Field Tracer Experiments

[8] A series of conservative tracer injections using sodium chloride (NaCl) were completed in 100 m “valley” reaches along the entire 2.8 km valley. We delineated reaches every 100 m along a straight line following the longitudinal axis of the valley rather than following the thalweg of the stream. Hereafter, we will refer to these as

stream reaches, or reaches, despite the fact that the actual channel length within the reach could be longer than 100 m. Using valley length to delineate reaches limits the potential for channel sinuosity to confound effects of lateral inputs on stream-groundwater interactions under different hydrological conditions. Similarly, gross losses to long residence time flow paths (i.e., spatial scales at the reach scale and larger) are likely to follow the valley axis rather than a sinuous stream channel. However, sinuosity was low throughout the entire study domain, so the difference between valley and channel-delineated stream reaches was usually small.

[9] Four sets of tracer injections were completed under four different base-flow conditions (ranging from 15 to 101 L s⁻¹ at the downstream end of the 2.8 km valley) to provide snapshots of solute transport during different hydrological conditions. In each injection, a known mass of solute was released as an instantaneous slug a mixing length upstream of the head of each reach. Studies were conducted during the periods 4–6 August 2005, 22–24 June 2006, 25–28 July 2006, and 26 August–4 September 2006, and tracer experiments were carried out only under base-flow conditions (i.e., when the stream flows were not influenced by infrequent summer rain fall). A mixing length is defined as the length of stream channel necessary to achieve well-mixed conditions in the vertical and transverse directions of the stream, determined here based on field observations of channel structure and ranged from 5 to 30 m [*Payn et al.*, 2009]. Prediction of mixing lengths by theoretical functions of channel morphology is not reliable in headwater mountain streams [*Day*, 1977]. Electrical

conductivity was used as a surrogate for tracer concentration in all measurements [after, for example, *Baxter et al.*, 2003; *Gooseff and McGlynn*, 2005; *Wondzell*, 2006]. In-channel electrical conductivity was recorded using Campbell Scientific loggers (Logan, Utah, USA), calibrated using known masses of NaCl and stream water. Additional details regarding the tracer injections can be found in *Payn et al.* [2009].

2.3. Unrecovered Tracer: Long-Term Storage

[10] Long-term storage calculations were completed using the channel water balance estimates described by *Payn et al.* [2009]. We used dilution gauging to calculate the discharge (Q , $\text{m}^3 \text{s}^{-1}$) at the downstream and upstream end of each reach. The net change in discharge (ΔQ , $\text{m}^3 \text{s}^{-1}$) was calculated using the difference between downstream and upstream discharges. Mass recovered at the downstream end of the reach was used to calculate mass loss in each reach. Assuming the only mechanism for mass loss is outflow from the channel (i.e., conservative behavior of the tracer, no loss due to instrument sensitivity) the gross losses of water from the channel can be calculated. End members to bound the range of possibilities can be calculated by assuming all loss occurs before gains (i.e., minimum dilution before loss; $Q_{\text{LOSS,MIN}}$, $\text{m}^3 \text{s}^{-1}$), or all gain before loss (i.e., maximum dilution before loss; $Q_{\text{LOSS,MAX}}$, $\text{m}^3 \text{s}^{-1}$) within a single study reach. Given the net change in discharge and gross losses, the associated end members of $Q_{\text{GAIN,MIN}}$ ($\text{m}^3 \text{s}^{-1}$) and $Q_{\text{GAIN,MAX}}$ ($\text{m}^3 \text{s}^{-1}$) can be calculated.

2.4. Recovered Tracer: Short-Term Storage

2.4.1. Window of Detection

[11] We sampled tracer concentrations until well after the stream returned to apparent background concentrations, and then calculated a maximum timescale of the observation (t_{99}) as the time elapsed from tracer first arrival to the time at which 99% of the recovered mass passed by the downstream observation point [after *Mason et al.*, 2012]. This choice is representative of the window of detection of the tracer injection, but eliminates subjectivity in choosing the time at which tracer is last present, as tailing may not be well observed using field probes [*Schmadel et al.*, 2011].

2.4.2. Temporal Moment Analysis of Tracer Breakthrough Curves

[12] Temporal moments are integrators of all physical processes affecting the observed breakthrough curve. In this case, the temporal moments integrate behavior of all mass recovered in the tracer study. For example, some degree of skewness can arise from an Eulerian simulation of advective and dispersive processes alone. Still, several studies have shown that temporal moments are useful for interpreting the relative importance of solute transport processes [e.g., *Schmid*, 2008; *Schmid*, 2003]. We used temporal moments to characterize the nature of solute residence time in each reach. In contrast to transient storage parameters, temporal moments of slug injection breakthrough curves are parameters of the statistical distribution of solute residence time in the reach, and were deterministically calculated directly from breakthrough curve data. Many studies have demonstrated the usefulness of breakthrough curve moment analysis in comparing the behavior

of different hydrologic systems [e.g., *Gupta and Cvetkovic*, 2000; *Schmid*, 2003]. We calculated the n th-order temporal moment (M_n) using:

$$M_n = \int_0^{t_{99}} C_{\text{norm}}(t) t^n dt \quad (1)$$

where t is time and $C_{\text{norm}}(t)$ represents the normalized, background-corrected concentration time series, and t_{99} is the time at which 99% of the recovered mass passes the observation point. The normalized concentration was calculated as:

$$C_{\text{norm}}(t) = \frac{C(t)}{\int_0^{t_{99}} C(t) dt} \quad (2)$$

where $C(t)$ is the observed tracer above background levels; all temporal moments are characterizations of only the recovered tracer mass. This normalization yields a zeroth temporal moment (M_0) of unity for all cases. The first temporal moment (M_1) is physically interpreted as the mean residence time. Higher-order central moments were calculated about the mean as:

$$\mu_n = \int_0^{t_{99}} C_{\text{norm}}(t) (t - M_1)^n dt \quad (3)$$

where μ_2 reflects the general spread of data round the mean residence time (temporal variance), and μ_3 reflects the skew in the data around the mean residence time [*Gupta and Cvetkovic*, 2000; *Harvey and Gorelick*, 1995]. Finally, we calculate skewness (γ , unitless) using the formal statistical definition.

$$\gamma = \frac{\mu_3}{\mu_2^{3/2}} \quad (4)$$

[13] We loosely interpret the magnitude of temporal moments and derived statistics as relative metrics of well known hydrologic processes. For example: the first moment is related to the influence of advection; the second is related to the influence of dispersion; and skewness is related to the influence of transient storage. However, direct quantification of these processes should not be inferred from this interpretation. As is evident in the parameter relationships derived by *Schmid* [2002] the value of a temporal moment is a complex function of more than a singular transient storage parameter.

2.4.3. Transient Storage Model Parameters

[14] Transient storage modeling was completed using the one-dimensional Transport with Inflow and Storage model [i.e., OTIS; *Runkel*, 1998]. In addition to limitations due to the study window of detection, discussed in the introduction, the transient storage model includes a number of assumptions that are limiting in its performance, including exponential residence time distribution in the storage zone, lumping of all storage as a single immobile domain, instantaneous well-mixed representation of mobile and immobile domains, and spatially uniform parameters within a reach. These limitations are well described in past studies [e.g., *Wagner and Harvey*, 1997]; for our purposes we use the widely applied single storage zone transient storage model presented by *Bencala and Walters* [1983], solved via the numerical scheme of *Runkel* [1998]. Furthermore, the

assumption of constant dispersivity required for the transient storage model may be inappropriate for mixing length stream tracer studies [Wang et al., 2011].

[15] Lateral inflow ($q_{L,in}$, $m^2 s^{-1}$) and outflow ($q_{L,out}$, $m^2 s^{-1}$) for each model reach were specified using arithmetic averages of maximum and minimum gross gains and losses, calculated as:

$$q_{L,in} = \frac{Q_{GAIN,MIN} + Q_{GAIN,MAX}}{2L} \quad (5)$$

and

$$q_{L,out} = \frac{Q_{LOSS,MIN} + Q_{LOSS,MAX}}{2L} \quad (6)$$

where L is the length of the experimental reach (m). Upstream boundary conditions were specified using the observed breakthrough curve at the upstream end of each reach.

[16] We completed 100,000 independent model runs as a Monte Carlo simulation, sampling the channel area (A), storage area (A_S), exchange coefficient (α), and dispersion coefficient (D) from uniform distributions (Table 1). Estimated channel area (A_{EST}) was calculated as

$$A_{EST} = \frac{Q_{AVG}}{V} \quad (7)$$

where Q_{AVG} is the average of the upstream and downstream discharges based on dilution gauging, and V is the advective velocity of the solute peak through the reach. The value for A_{EST} was used to constrain the range of areas explored using the equation (Table 1). For all parameters, minimum and maximum values are summarized in Table 1. The quality of fit for each simulation was calculated using a root mean square error (RMSE) criterion comparing the simulated breakthrough curve to the observed downstream breakthrough curve. We compare inferred hydrologic characteristics of reaches across space and time using the parameter set with the lowest RMSE value for each reach and tracer experiment. We also calculated the coefficient of variation (CV) for each parameter across the parameter sets that generated the 100 lowest RMSE values out of the 100,000 model runs (i.e., lowest 0.1% of RMSE values). We interpret the CV as a relative metric of our ability to extract information from a given tracer experiment with the model, where a lower CV for a given parameter means the tracer data provided more information about that parameter

[17] Finally, we calculated the fraction of median transport time for a 200 m reach due to transient storage after Runkel's [2002] empirical relationship

$$F_{med}^{200} \cong (1 - e^{-L\frac{\alpha}{A+A_S}}) \quad (8)$$

[18] The value of F_{med}^{200} is highly dependent on reach length, so it is normalized to a 200 m reach to allow inter-site comparison of results. We use this as a relative metric of the influence of transient storage that is independent of tradeoffs between A_S and α .

2.5. Organization of Short- and Long-Term Storage Relationships With Discharge

[19] To quantify relationships between discharge and solute transport processes and metrics, we used Pearson's correlation coefficient. Additionally, p values were calcu-

Table 1. Parameter Ranges Considered for the Monte Carlo Simulation

Parameter	Minimum Value	Maximum Value
A (m^2) ^{a,b}	$0.5 \times A_{EST}$	$1.5 \times A_{EST}$
A_S (m^2) ^c	1×10^{-2}	10
α (s^{-1}) ^c	1×10^{-8}	1×10^{-1}
D ($m^2 s^{-1}$) ^c	1×10^{-4}	5

^aThe estimated cross-sectional area (A_{EST}) was based on average discharge at the head of the reach divided by velocity (determined by time elapsed between upstream and downstream peaks for each tracer injection). Monte Carlo parameter sampling was random and unstratified.

^bLinear spacing.

^cLogarithmic spacing (i.e., equal representation of each log cycle).

lated to test the null hypotheses of no correlation. Correlation coefficients and p values were calculated using MATLAB (The MathWorks, Inc., Natick, MA). Negative gross gains and positive gross losses are considered as errors with no physical explanation and were omitted from calculations to avoid noninterpretable bias in correlation coefficients.

[20] Linear correlation coefficients were used to interpret the effects of discharge variability in both space and time. First, we grouped data temporally by the hydrologic conditions during which they were collected, such that we compared variability in discharge along the reach to the corresponding variability in solute transport metrics at a given discharge condition. This analysis was designed to assess the potential effect of spatial variability in discharge on the spatial organization of solute transport metrics. Second, we grouped data by location along the valley, such that we compared variability in discharge through time to the corresponding variability in solute transport metrics at a given location along the valley. This analysis allows us to assess the potential effect of temporal variability in discharge on the temporal organization of solute transport metrics, and how those effects may vary along the valley. For the second analysis, we avoided bias from insufficient data by only using locations where at least 3 data points exist, because two data points always yields perfect correlation. In this study, we interpret only the sign of these correlation coefficients, given that the low number of data points does not support a rigorous statistical interpretation.

2.6. Spatial and Temporal Scales of Short-Term Storage

[21] To determine the spatial scale of flow paths that could reasonably be detected, we estimated subsurface velocities using Darcy's law

$$V_{SUB} = \frac{K}{\eta} S \quad (9)$$

where V_{SUB} is the subsurface velocity of water moving through pore spaces ($m s^{-1}$), K is the hydraulic conductivity ($m s^{-1}$), η is porosity, and S is the hydraulic gradient ($m m^{-1}$). Then we calculated a characteristic maximum flow-path length using t_{99} , the characteristic time scale for short-term storage.

$$L_C = V_{SUB} t_{99} \quad (10)$$

[22] We assumed subsurface properties of $K = 1.0 \times 10^{-4} m s^{-1}$ and $\eta = 0.25$, representative of a clean sand. These

assumptions should be conservative in that our estimates are likely to result in a faster estimated Darcian flow than is likely to occur in the field (excepting preferential flow paths) because the observed sediment textures included substantial amounts of silt and clay which should result in a K substantially lower than that of a clean sand and possibly higher porosity. Consequently, the spatial scales we calculated are likely to be longer than those actually found in the field. Additionally, we assumed the average hydraulic gradient in the reach can be approximated by the valley slope between the upstream and downstream monitoring locations, based on topographic survey of the site [after *Wondzell*, 2011]. These estimates are based on the assumption that the temporal scale of the longest flow path to which our experiment is sensitive would be no longer than t_{99} for a study. This equivalent length metric is useful to conceptualize the maximum spatial scales of flow paths sampled in our study, though we acknowledge that its magnitude is subject to several simplifications that may be inaccurate. This analysis is akin to the hyporheic potential described by *Wondzell* [2011].

3. Results

3.1. Long-Term Storage

[23] Most reaches had substantial simultaneous gains and losses relative to upstream flow during lower discharge conditions (Figure 2). Gains near the tributary at 2200 m can be clearly observed during the three highest discharge conditions. The largest net gains were downstream of the valley transition at 1200 m; visible perennial seeps and springs suggest a substantial source of lateral groundwater inputs in this region [*Jencso et al.*, 2010; *Payn et al.*, 2012]. As in the earlier analysis of these data performed by *Payn et al.* [2009], the magnitude of bidirectional exchange in the system generally increased between high base-flow and intermediate or low base-flow studies. At the lowest discharge condition, the stream reaches from 900 to 1100 m exhibited gross gains and losses that were anomalously large relative to the rest of the stream channel.

[24] During the four base-flow conditions, both positive and negative correlations were found between discharge and gross gains (Table 2). Both minimum and maximum gross losses were negatively correlated with flow during the two highest-flow conditions, but the relationship switches sign for the maximum gross loss under the lowest-flow conditions (Table 2). Most individual reaches demonstrate positive correlations between flow and gross gains and negative correlations between flow and gross losses (Table 3). The 1300 and 1900 m reaches demonstrate the opposite relationship between discharge and gross gains. Increases in stream flow were generally associated with increasing magnitudes of gross gains and losses.

3.2. Short-Term Storage

3.2.1. Spatial and Temporal Trends in Temporal Moments of Tracer Breakthrough Curves

[25] In general, mean residence time and temporal variance are largest for the spatial locations and hydrological conditions with lowest discharges (Figure 3). Higher order central moments (μ_3 and μ_4 , not shown here) represent similar trends to those observed in μ_2 , with the higher moments

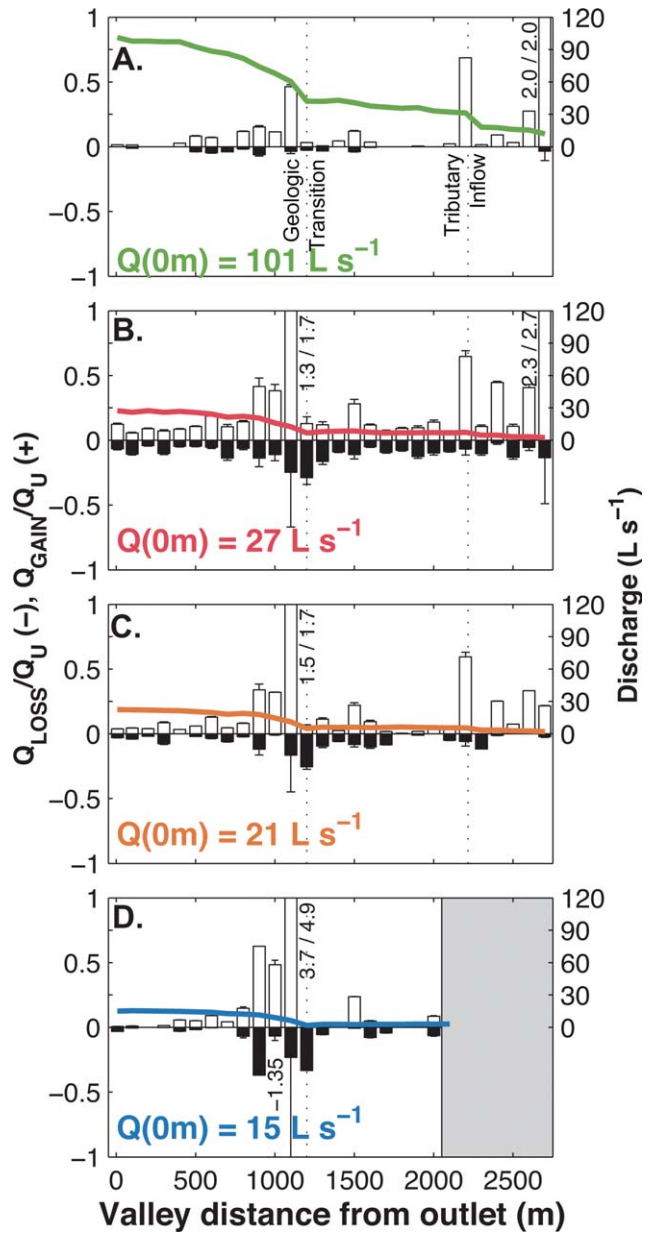


Figure 2. Gross gains and losses for 100 m reaches under four-flow conditions, normalized by flow at the upstream end of the reach. Plots are sorted from the highest to lowest discharge at the downstream extent of the study. Spatial patterns in discharge during each set of injections are shown as the solid line (right-hand Y-axis). Bar heights and single-sided error bars represent the minimum and maximum, respectively, gross gains (Q_{GAIN}) and losses (Q_{LOSS}) normalized by upstream discharge in the reach (Q_U). The shaded portion in the bottom subplot represents locations where data were unavailable due to very low flow in the channel.

amplifying different features of each distribution. Skewness is generally largest for the highest discharge locations and conditions, though substantial noise exists in this relationship (Figure 3). Temporal moments demonstrate a

Table 2. Sign of Linear Correlation Coefficient Values (R) for In-Stream Discharge and Metrics of Long- and Short-Term Storage^a

	$Q_{GAIN,MAX}$	$Q_{GAIN,MIN}$	$Q_{LOSS,MAX}$	$Q_{LOSS,MIN}$	M_1	μ_2	γ	A	D	A_S	α
$Q(0)=101 \text{ L s}^{-1}$	(+)	(+)	(-)	(-)	(-)	(-)	(-)	(+)	(+)	(-)	(+)
$Q(0)=27 \text{ L s}^{-1}$	(+)	(+)	(-)	(-)	(-)	(-)	(-)	(+)	(+)	(+)	(+)
$Q(0)=21 \text{ L s}^{-1}$	(+)	(+)	(-)	(-)	(-)	(-)	(-)	(+)	(+)	(+)	(+)
$Q(0)=15 \text{ L s}^{-1}$	(-)	(-)	(+)	(-)	(-)	(-)	(-)	(+)	(+)	(+)	(-)

^aData for each base-flow condition (all spatial locations) were considered together for this analysis. Values of (+) indicate increasing value with increasing discharge; (-) indicates decreasing value with decreasing discharge.

generally consistent pattern with discharge, whether discharge varies in space or time.

[26] For all flow conditions, mean residence time was negatively correlated with the variability in flow along the stream (Table 2), which may be expected as velocity and flow rate are related. Mean residence time was also negatively correlated with discharge at all sites through time (Table 3). Variance (μ_2) was also negatively correlated with the variability in flow across both space and time (Tables 2 and 3). Skewness (γ) was negatively correlated with variability in discharge along the reach for all base-flow conditions (Table 2), and positively correlated with discharge for 22 of 28 spatial locations (Table 3). Results in Table 2 suggest that while predictable relationships with flow are apparent in temporal moments (Figure 3), relationships between these statistical descriptions of solute transport and flow are highly variable on a reach-by-reach basis (likely due to heterogeneity in the system). At a more coarse scale, increasing flow rates generally yielded a decrease in skewness with space, but the trend did not hold

at individual reaches considered under different discharges. This is likely because lower flow is associated with lower velocity, and more time for processes other than advection to affect the solute signal. In an independent analysis of the same data, *Patil et al.* found that differences in short-term storage were associated with changes in stream morphology (shorter tails in downstream reaches, where there is a steeper slope, decreased sinuosity, and granite-gneiss bedrock) during the lowest discharge conditions. These conclusions, however, attribute the changes to both the physical system and the increased discharge and velocity in downstream reaches. Although the physical system changes in the valley bottom (slope, sinuosity, underlying geology), *Patil et al.* were unable to parse these controls from the discharge and velocity differences along the reach.

3.2.2. Spatial and Temporal Trends in Transient Storage Model Parameters

[27] Best fit transient storage model parameters fit observations reasonably well (RMSE 0.22–6.24, mean 1.61). As would be predicted by simple scaling relationships

Table 3. Sign of Linear Correlation Coefficient Values (R) for In-Stream Discharge and Metrics of Long- and Short-Term Storage^a

Distance From Valley Outlet (m)	$Q_{GAIN,MAX}$	$Q_{GAIN,MIN}$	$Q_{LOSS,MAX}$	$Q_{LOSS,MIN}$	M_1	μ_2	γ	A	D	A_S	α
7	(+)	(+)	(-)	(-)	(-)	(-)	(+)	(+)	(+)	(-)	(-)
100	(+)	(+)	(-)	(-)	(-)	(-)	(+)	(+)	(+)	(-)	(-)
200	--	--	--	--	(-)	(-)	(-)	(+)	(-)	(+)	(+)
300	(+)	(+)	(-)	(-)	(-)	(-)	(+)	(+)	(-)	(+)	(+)
400	(+)	(+)	--	--	(-)	(-)	(+)	(+)	(+)	(+)	(+)
500	(+)	(+)	(-)	(-)	(-)	(-)	(+)	(+)	(+)	(-)	(+)
600	(+)	(+)	(-)	(-)	(-)	(-)	(-)	(+)	(+)	(+)	(+)
700	(+)	(+)	(-)	(-)	(-)	(-)	(-)	(+)	(-)	(+)	(+)
800	(+)	(+)	(-)	(-)	(-)	(-)	(+)	(+)	(+)	(+)	(+)
900	(+)	(+)	(-)	(-)	(-)	(-)	(+)	(+)	(-)	(-)	(-)
1000	(+)	(+)	(-)	(-)	(-)	(-)	(-)	(+)	(+)	(-)	(+)
1100	(+)	(+)	(+)	(-)	(-)	(-)	(+)	(+)	(+)	(-)	(+)
1200	(+)	(+)	(+)	(+)	(-)	(-)	(+)	(+)	(+)	(+)	(+)
1300	(-)	(-)	(-)	(-)	(-)	(-)	(+)	(+)	(+)	(+)	(+)
1400	(+)	(+)	--	--	(-)	(-)	(+)	(+)	(+)	(+)	(+)
1500	(+)	(+)	(-)	(-)	(-)	(-)	(-)	(+)	(+)	(-)	(-)
1600	(+)	(+)	(+)	(+)	(-)	(-)	(+)	(+)	(+)	(+)	(-)
1700	(+)	(+)	(-)	(-)	(-)	(-)	(+)	(+)	(+)	(+)	(+)
1800	--	--	--	--	(-)	(-)	(+)	(+)	(+)	(+)	(+)
1900	(-)	(-)	--	--	(-)	(-)	(+)	(+)	(-)	(+)	(+)
2000	(+)	(+)	--	--	(-)	(-)	(+)	(+)	(+)	(+)	(-)
2100	(+)	(+)	--	--	(-)	(-)	(+)	(+)	(-)	(-)	(+)
2200	(+)	(+)	--	--	(-)	(-)	(+)	(+)	(+)	(+)	(-)
2300	--	--	--	--	(-)	(-)	(+)	(+)	(+)	(-)	(-)
2400	(+)	(+)	--	--	(-)	(-)	(+)	(+)	(+)	(-)	(-)
2500	(+)	(+)	--	--	(-)	(-)	(+)	(+)	(+)	(-)	(-)
2600	(+)	(+)	--	--	(-)	(-)	(+)	(+)	(+)	(-)	(+)
2700	(+)	(+)	(-)	(-)	(-)	(-)	(-)	(+)	(+)	(-)	(+)

^aData from all four base-flow conditions at a single reach were combined for this analysis. Values listed as "--" represent locations where no analysis was completed due to less than three physically meaningful points were collected (e.g., positive losses and negative gains were considered not physical and were omitted from the study). Values of (+) indicate increasing value with increasing discharge; (-) indicates decreasing value with decreasing discharge.

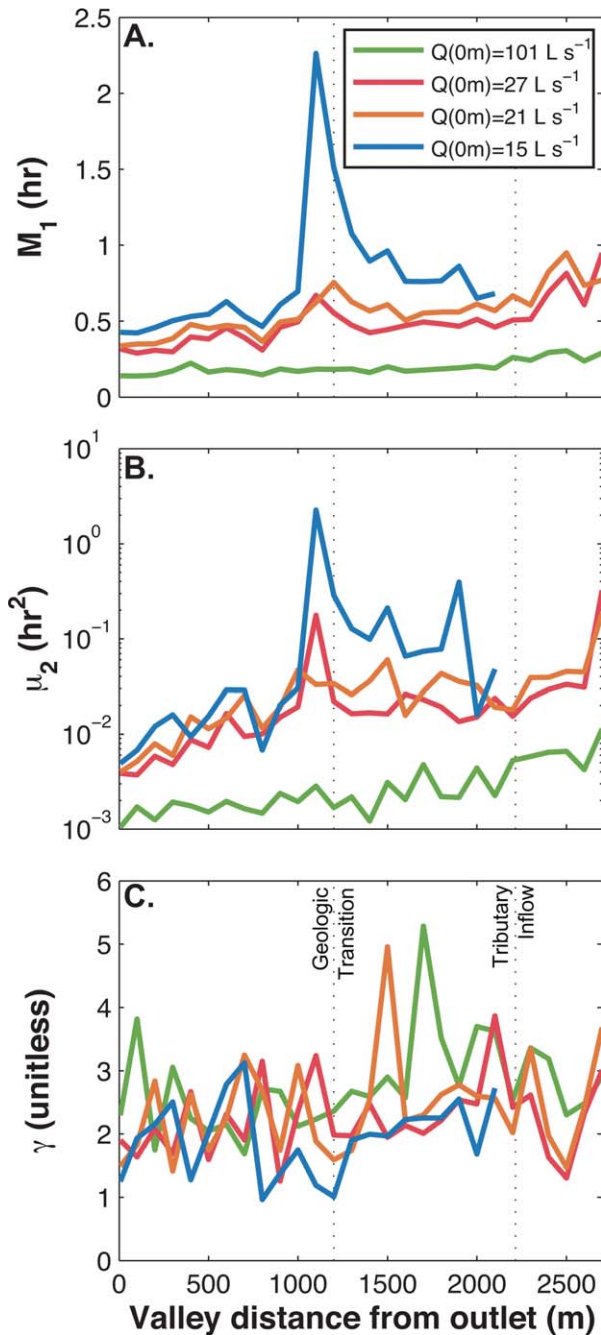


Figure 3. Temporal moment analysis of the recovered tracer at the downstream end of each 100 m reach, under four hydrological conditions. Mean residence time (M_1) is generally longest in locations and under conditions with the lowest flow rates. Variance (μ_2) is typically largest for the reaches with the lowest discharge along the stream, and for the lowest flow conditions in individual reaches. No discernable pattern in space or between base-flow conditions is observed for skewness (γ).

[e.g., Leopold and Maddock, 1953], values of A generally decreased with decreasing discharge, both along the stream and with seasonal recession (Figure 4A). For D , A_S , and α , no discernable trends in space nor with base-flow recession were observed (Figures 4B–D). Based on the parameter CV

across the 100 lowest RMSE values (RMSE 0.58–12.34, mean 3.15 for parameter sets considered), the model and tracer data generally provided the most information about A (CV of $\sim 32\%$ for most tracer studies), followed by A_S , D , and α (Figure 4E–H). Other than some apparent outliers, CV values for individual parameters were generally invariant with respect to both reach location and discharge condition. Values for D , A_S , and α have large CV values (about 220%, 150%, and 280%, respectively), suggesting there is substantially less information about these parameters in the tracer data. This is expected given several past studies reporting similar findings, and is likely caused by interaction between these three parameters to produce similar tailing behavior of the breakthrough curve [e.g., Mason *et al.*, 2012; Lees *et al.*, 2000; Wagner and Harvey, 1997]. The CV values found in this study were considered too large to produce meaningful estimates of the numerous metrics describing transient storage by combination of transient storage model parameters (e.g., the average residence time of a particle within the storage zone, commonly T_{sto} , after Thackson and Schnelle [1970]). For this manuscript, we continue exploration of recovered tracer data using a single parameter set that provides the best fit for each reach (rather than considering a range of values), as is commonplace with results of other parameter fitting tools and transient storage modeling in general. This provides some common context with a multitude of past transient storage studies. However, the apparent lack of information indicated by high-CV values suggests that our attempt to identify α and A_S from these tracer data is suspect. We leave more detailed analysis of the identifiability of transient storage model parameters for future study (see C. A. Kelleher *et al.*, Identifiability of transient storage model parameters along a mountain stream, submitted to *Water Resources Research*, 2013), but we suggest that more studies of transient storage should include a check on parameter identifiability, as we have provided here.

[28] During all base-flow conditions, variability in A was positively correlated with the variability in Q along the stream (Table 2). For all stream reaches, variability in A was also positively correlated with the variability in Q through time (Table 3). Dispersion was positively correlated with discharge for all base-flow conditions (Table 2). Dispersion and discharge were positively correlated for 22 of 28 spatial locations, though negative correlations exist for some spatial segments. There were no patterns evident in the spatial (Figure 3) or temporal (Figure 4) correlations of A_S and α with discharge.

3.2.3. Expected Relationships Between Short-Term Storage and Temporal Moments

[29] Although temporal moments cannot be directly mapped to physical processes, some relationships are expected to exist. Because M_1 is a description of advective timescale, which is related to both Q and A , we expect a relationship to exist between A and M_1 . This relationship is apparent in our data set, with the longest advective timescales associated with smaller streams (i.e., locations with lower discharge; Figure 5A). Spreading of tracer along the longitudinal axis of the stream would be evidenced by temporal variance (μ_2) in the downstream signal; we expected the largest dispersion coefficients would be associated with the largest discharges due to increased turbulence in the

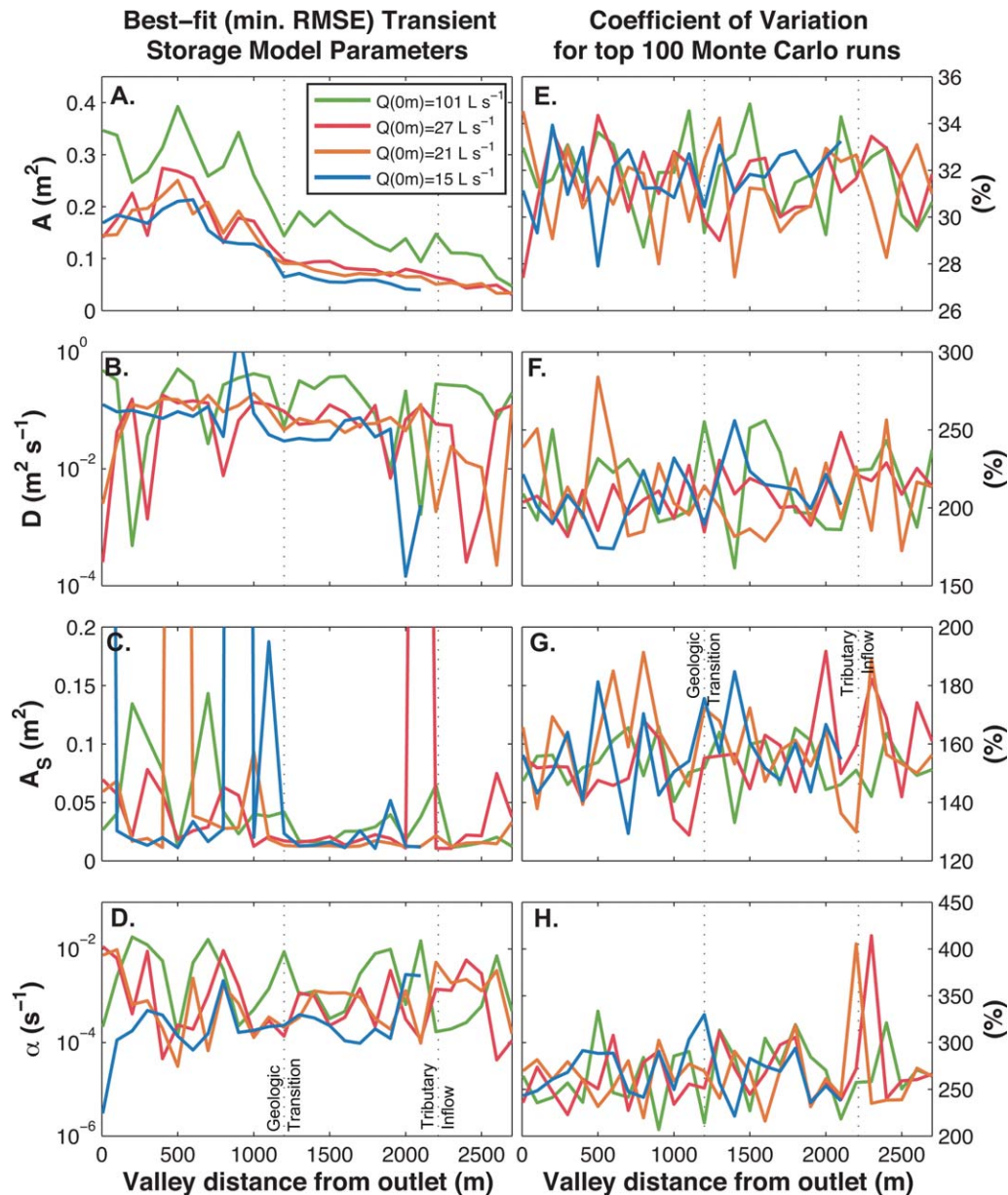


Figure 4. Spatial distribution of transient storage parameters channel area (A), dispersion (D), storage area (A_S), and exchange coefficient (α), determined by the minimum RMSE from the 100,000 Monte Carlo simulations for each slug injection (left column) and the coefficient of variation (i.e., noise-to-signal ratio, calculated as standard deviation normalized by mean) for the 100 lowest RMSE parameter sets.

stream during greater discharges. The largest values for variance are associated with the lowest discharges. We found this trend to generally hold true (Figure 5B). No trend between temporal variance and dispersion coefficient was observed because the dispersion coefficient is a function of the physical system, while temporal variance is dependent upon travel time in the reach (i.e., longer t_{99} results in more time for processes other than advection to act on the input signal). Finally, skewness measures the asymmetry of the distribution (more positive representing increased tailing). In our study, we expect that increased skewness would be associated with increased transient storage of solutes. The metric F_{med}^{200} was developed to provide a quantification of transient storage that is independent of

recognized tradeoffs between A_S and α in the transient storage model parameters [Runkel, 2002]. Little pattern is observed here between skewness and F_{med}^{200} (Figure 5C). Taken together, results in Figure 5 suggest that transient storage model parameters describing exchange (A_S and α) were not related to the statistical description of the distribution that is most sensitive to transient storage (skewness), though both advective timescales and dispersion are at least weakly related to their associated temporal moments.

3.3. Linking the Window of Detection With Short- and Long-Term Storage

[30] In our study, t_{99} ranges from about 0.3 to 6.2 h (Figure 6). Across the hydrologic conditions observed in

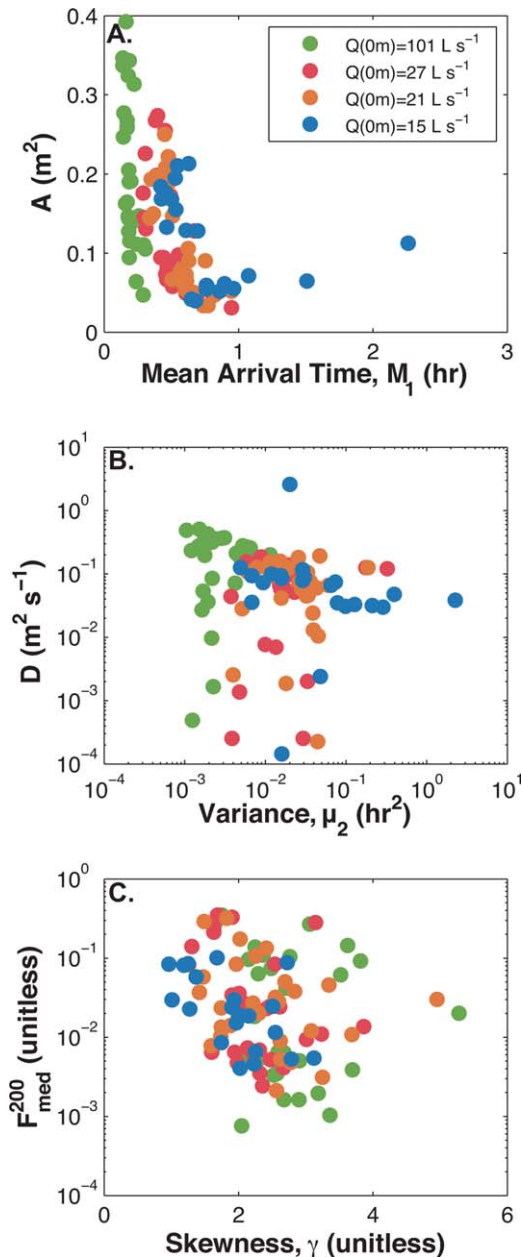


Figure 5. (A) Mean residence time and area (A) exhibit an inverse relationship. This is expected because increasing area is associated increasing flow rate and increasing velocity, which would decrease the advective timescale of transport. (B) Variance represents a spreading of the solute tracer signal in time, expected to arise primarily due to dispersion (D) along the longitudinal axis of the stream. Indeed, the variance in the recovered solute tracer signals are generally associated with the largest dispersion coefficients. (C) Although a positive relationship is expected between F_{med}^{200} (which quantifies transient storage by combining both exchange rate and storage area as a single metric) and skewness, the data present no obvious trend.

this study, the window of detection in individual reaches changed by an average of 1.4 h (with observed ranges of 0.4 at the catchment outlet to 5.8 h at the location of the geologic transition, near 1200 m). The methods used in

this study directly limit the suite of flow paths that can be characterized as short-term storage flow paths (i.e., those described by the transient storage model). The window of detection in solute tracer studies directly limits the temporal scale of flow paths that can be observed, and preferentially samples only the fastest flow paths [e.g., Harvey *et al.*, 1996; Harvey and Wagner, 2000].

[31] In general, slug injections in reaches with lower discharge are sensitive to longer residence time flow paths relative to the same reach in higher discharge conditions due to their longer window of detection and slower down-valley velocity (Figure 6). Analysis of the window of detection as a function of discharge shows an inverse relationship between stream discharge and window of detection (Figure 6). These results are consistent with predictions on the window of detection limitations in solute tracer studies [Harvey *et al.*, 1996; Wagner and Harvey, 1997; Harvey and Wagner, 2000].

[32] Considering results of all tracer studies together, weak relationships are present for increases in tracer mass loss, decreases in gross gains, and decreases in gross losses are observed with increasing t_{99} (Figure 7). Examining data from individual sets of tracer experiments does not show any relationship between tracer mass loss, gross losses, or gross gains and t_{99} . While there may be possible hydrological explanations for these patterns we also caution that the interpretation of these relationships is confounded by the interaction of stream velocity, tracer dilution, and instrument sensitivity, given the wide range in discharges across which the tracer injection experiments were conducted.

[33] Comparison of t_{99} and temporal moments show power law trends (Figure 8), which were also reported by Schmid's [1995] numerical simulations. Central moments of higher order (μ_3 and μ_4) show similar trends to those presented for μ_2 . Skewness (γ) does not show a strong relationship with t_{99} in our study. Visually, A has the strongest relationship with t_{99} of any of the transient storage parameters (Figure 9), which is expected since the stream's cross-sectional area, discharge, and velocity are typically related [e.g., Leopold and Maddock, 1953], and relationships between t_{99} and discharge (Figure 6) have already been demonstrated. Weak correlations may be present between other transient storage model parameters and t_{99} (Figure 9), but uncertainty in parameter identification and equifinality in the transient storage model framework overwhelm our ability to identify meaningful relationships between these parameters and the physical system [Marion *et al.*, 2003; Wondzell, 2006].

4. Discussion

4.1. The Window of Detection Is a Primary Control on Interpretation of Solute Tracer Studies

[34] Solute tracer studies have been widely applied in a wide range of stream types and sizes, but all suffer from one fundamental problem: how do we interpret the results of these data, given critical limitations in our knowledge of the physical system, ability to represent that knowledge in a modeling framework, and ability to uniquely parameterize the model? Of fundamental importance is the window of detection associated with individual solute tracer studies. First, injections with a longer t_{99} exhibit more tailing in short-term storage and both greater gross gains and losses. Such results might be expected. As advective travel time

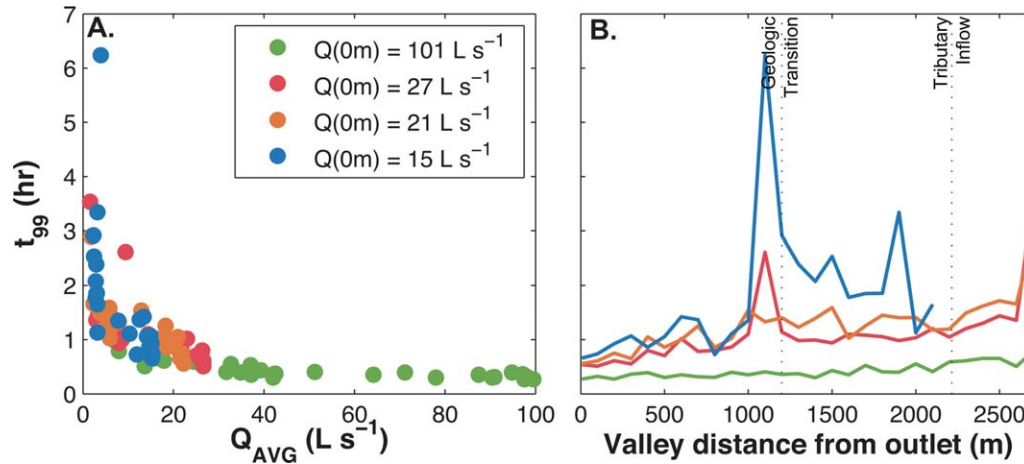


Figure 6. Time elapsed to 99% of recovered tracer passage (t_{99}) as a function of (A) average discharge in the reach (Q_{AVG}) and (B) valley distance from outlet. The window of detection is related to discharge, the primary control on transport time through a stream reach.

through the reach slows (larger t_{99}) more tracer-labeled water would be lost from the channel (i.e., there is more time for processes other than advection to affect the solute pulse, the main premise of several past studies [Harvey *et al.*, 1996; Wagner and Harvey, 1997; Harvey and Wagner, 2000]). For example, we might expect that, in stream reaches where gross gains come from localized hillslope hollows, gross gains might decrease with decreasing discharge, because both streamflow and hillslope-sourced inputs should decline as the catchment dries and water stored in hillslopes is depleted. As lateral inputs decrease, head gradients might be reversed in the shallow riparian aquifer, at least some locations, such that water tables slope away from the stream and allow greater gross losses. We also see that gross gains are constant or possibly increase as t_{99} increases. Again, this relationship might be expected. The largest gross gains are in the region 1200 m from the mouth of the stream, at the contact zone between the overlying sandstones and deeper confining layers. This portion of the stream appears to be a major groundwater discharge zone from larger, more spatially extensive aquifers (as opposed to hillslope-sourced water from soils in hillslope hollows). Thus, it might be reasonable to expect that groundwater discharge from such an aquifer would not be very sensitive to seasonal changes in catchment wetness. Thus, as streamflow decreases through the period of summer base-flow recession, these groundwater inflows become larger and larger relative to the declining stream flow.

[35] The problem with these explanations, however, is that our measures of both short- and long-term storage are functions of tracer study design. Thus we are unable to isolate the influence of potential physical changes in the catchment hydrology from the influence of flow velocity on the advective time scale, which should also lead to an increase in the relative magnitude of both gross gains and losses as t_{99} increases. Our results support the earlier observations by Harvey *et al.* [1996], Wagner and Harvey [1997], and Harvey and Wagner [2000]—the window of detection differences confound results of any study designed around comparisons among replicated stream tracer injection experiments.

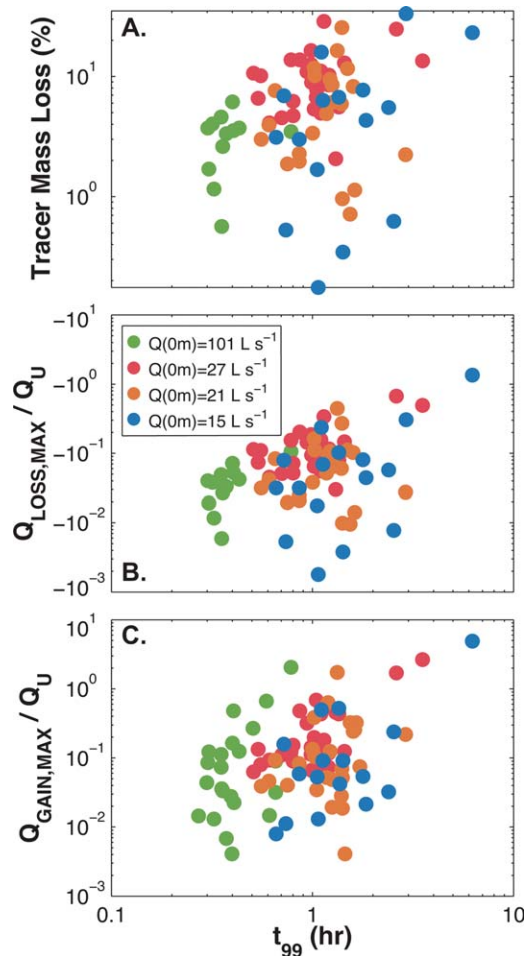


Figure 7. Tracer window of detection (t_{99}) as a control on metrics of long-term storage including (A) tracer mass loss, (B) gross loss ($Q_{LOSS,MAX}$), and (C) gross gain ($Q_{GAIN,MAX}$) as a fraction of discharge at the upstream end of each study reach (Q_U).

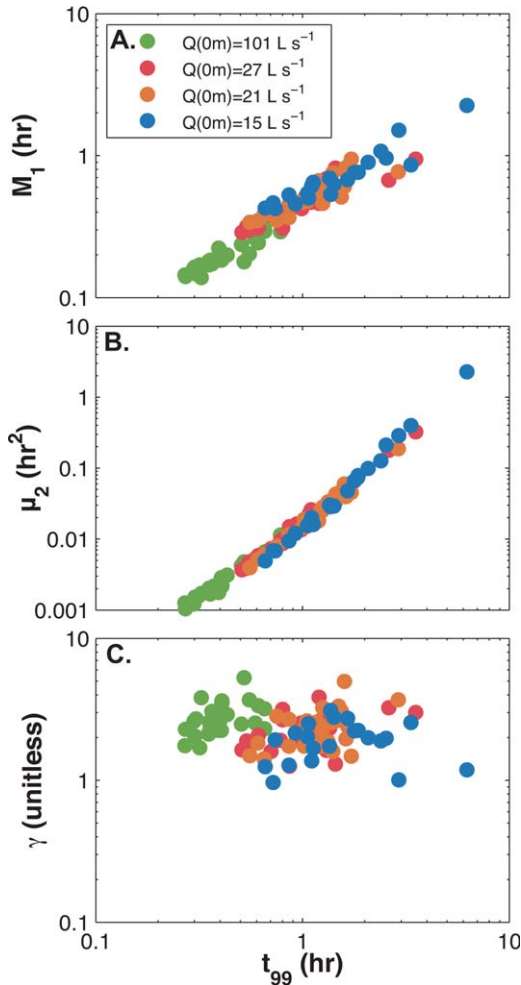


Figure 8. Tracer study window of detection as a control on (A) mean arrival time (M_1), (B) temporal variance (μ_2), and (C) skewness (γ). The measure of tailing in the studies, skewness, is independent of the window of detection.

[36] The attributes of the breakthrough curve captured by temporal moments are different than those aspects captured by calculating gross gains and losses, and also different from the transient storage model parameters. That so many of these parameters are sensitive to t_{99} (our proxy for the size of the window of detection) suggests that the issue lies fundamentally with the physical behavior of the tracer plume as it is transported downstream and is not simply an artifact of the analytical method used to analyze the shape of the breakthrough curve. Thus, slower advective transport and larger t_{99} give more time for dispersive and other physical processes to operate on the input signal as it moves through the reach. Each tracer breakthrough curve, therefore, represents a unique subset of physical processes in the reach that act upon the input signal. The window of detection is a unique to each combination of study reach, hydrologic state, and methodology; as such, the window of detection serves as a conceptual boundary between short- and long-term storage, but one that is difficult to compare between experiments.

4.2. Coupled Interpretation of Short- and Long-Term Storage

[37] To explicitly compare fluxes associated with short- and long-term storage for each study, we used the best fit parameter set to calculate the hyporheic exchange flux at the scale of each study reach (Q_{HEF}) as, $Q_{HEF} = L\alpha A$ [after Harvey and Wagner, 1996]. Most tracer releases show larger magnitudes of Q_{HEF} than $Q_{LOSS,MAX}$ (Figure 10); we found no explicit pattern in space, with discharge, or with t_{99} . Based on this analysis, we conclude that the

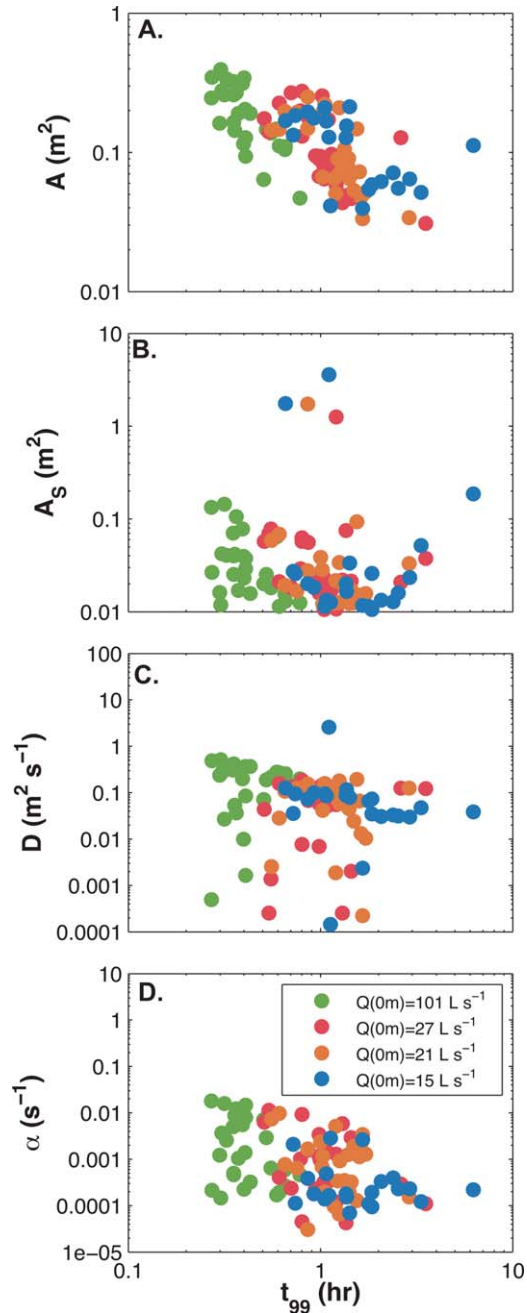


Figure 9. Tracer study window of detection as a control on transient storage model parameters (A) channel area, (A); (B) storage area, (A_s); (C) dispersion, (D); and (D) exchange coefficient, α .

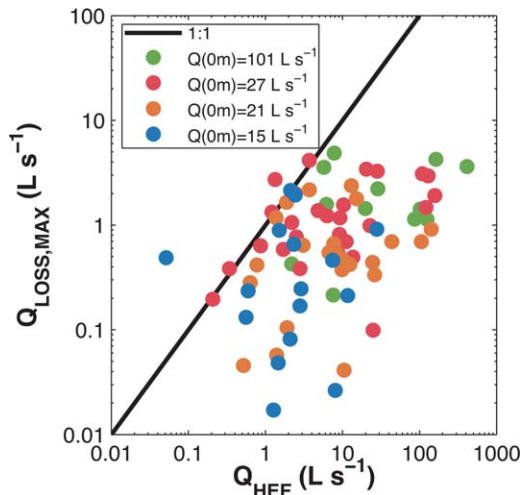


Figure 10. A comparison of fluxes of water through short-term storage (Q_{HEF}) and long-term storage (as $Q_{\text{LOSS,MAX}}$). Short-term storage flux generally dominates in this study, and is independent of long-term storage fluxes.

observation of short-term storage cannot be used as a surrogate to explain or quantify long-term storage, and vice versa (i.e., increasing magnitudes of long-term storage do not necessarily indicate increased nor decreased short-term storage, although both describe fate of solutes beyond the advection-dominated main channel). The two are different suites of physical processes separated conceptually by the t_{99} for the study. Consequently, the distinction of short- and long-term storage primarily becomes a function of the study design under the hydrologic conditions that were present at the time of the tracer injection. Changing either the study design or the hydrologic conditions changes the underlying time scale so that short- and long-term storage become highly variable in both space and time. However, since the processes do differentiate two temporal scales of observation (albeit separated by an arbitrary boundary arising from the method, t_{99}), there may be utility in computing both measures if they can contribute to a more complete understanding of solute transport through streams. Coupled interpretation of short- and long-term storage allows a distinction to be drawn between short- and long-term storage. Although these two categories are coarse in their characterization, and likely include a high degree of heterogeneity within each category, the ability to differentiate between broad categories of flow paths provides insight that has heretofore been unavailable based on field studies.

[38] We characterized the spatial and temporal scales of short-term storage using a simplified analysis based on hyporheic potential [after *Wondzell, 2011*]. The observed t_{99} 's ranged from 0.3 to 6.2 h, corresponding to flow paths ranging in length from 0.04 to 0.89 m. Thus, the flow paths observed in recovered tracer either represent storage in the surface stream channel or very short hyporheic exchange flow paths such as those flowing under a few cobbles or through small bed forms that might be found at a small vertical step in the channel or through a tiny gravel bar (on the order of 10^4 s, Figure 11). While the structure of Figure 11 [after *Harvey and Wagner, 2000*] presents spatial and temporal scales of subsurface flow paths, we emphasize that

our results are also sensitive to in-stream storage (e.g., recirculating eddies or other in-stream “dead zones”) rather than in subsurface flow paths; we do not have the ability to differentiate between surface and subsurface domains based on the data collected, and lump all fates into short-term storage in this manuscript. Flow paths occurring at longer temporal scales (irrespective of their spatial scale) are categorized as long-term storage (in our study, $t_{99} > \sim 5$ h, the upper section of Figure 11). Finally, flow paths with temporal scales within the window of detection but in locations that bypass the downstream observation point violate the assumptions of the transient storage modeling framework. Because flow paths visible within the window of detection are so short (< 1 m by our calculations, Figure 11), only a small amount of stream water would be expected to infiltrate into the streambed in the last meter of the study reach, so these bypass flows should not contribute substantially to measured long-term storage. As a thought exercise, consider a 100 m stream reach with homogeneous and isotropic subsurface. Flow paths must return to the channel within 1 m of the point at which they leave the channel based on our observed t_{99} and Darcy's Law assumptions. As such, bypass flows included in long-term storage can represent no more than 1 m of the total 100 m reach (i.e., 1% of the gross losses).

4.3. Organization of Short- and Long-Term Storage With Discharge

[39] The objective of this study was to determine if stream discharge is a primary factor in establishing short- and long-term storage of solutes and water along the longitudinal axis of a mountain headwater valley, as suggested by other studies [*Wondzell, 2011, 2012; Jin and Ward, 2005; Covino et al., 2011; Butturini and Sabater, 1999; Fabian et al., 2011; Hart et al., 1999; Karwan and Saiers, 2009; Morrice et al., 1997; Schmid, 2008, 2010; Wondzell, 2006; Zarnetske et al., 2007*]. Results of this study do not support a general relationship between discharge and short- or long-term storage along the longitudinal axis of the stream, considering individual sets of injections (conducted under four base-flow conditions). For the spatially explicit analysis (i.e., reach-by-reach), we conclude that although recovered tracer exhibits some organization (e.g., M_1, μ_2), no consistent and robust relationships were present for metrics quantifying short- or long-term storage. Given the variability in sign of correlation, we conclude transient storage model parameters are not well linked to stream discharge at individual reaches. Finally, no discernable shift in organization of short- or long-term storage under different base-flow conditions was apparent in our study. We conclude that our interpretations of short- and long-term storage do not vary systematically with decreasing base-flow conditions.

4.4. Implications for Replicate and Synoptic Studies

[40] Based on our analysis of short- and long-term storage in 28 contiguous reaches along a valley floor, we conclude that each reach and hydrologic condition is a unique filter that acts upon the input signal of the solute tracer [supporting the conceptualization of, for example, *Harvey and Wagner, 2000*]. From these results, we posit that heterogeneity along the valley at scales smaller than observed in

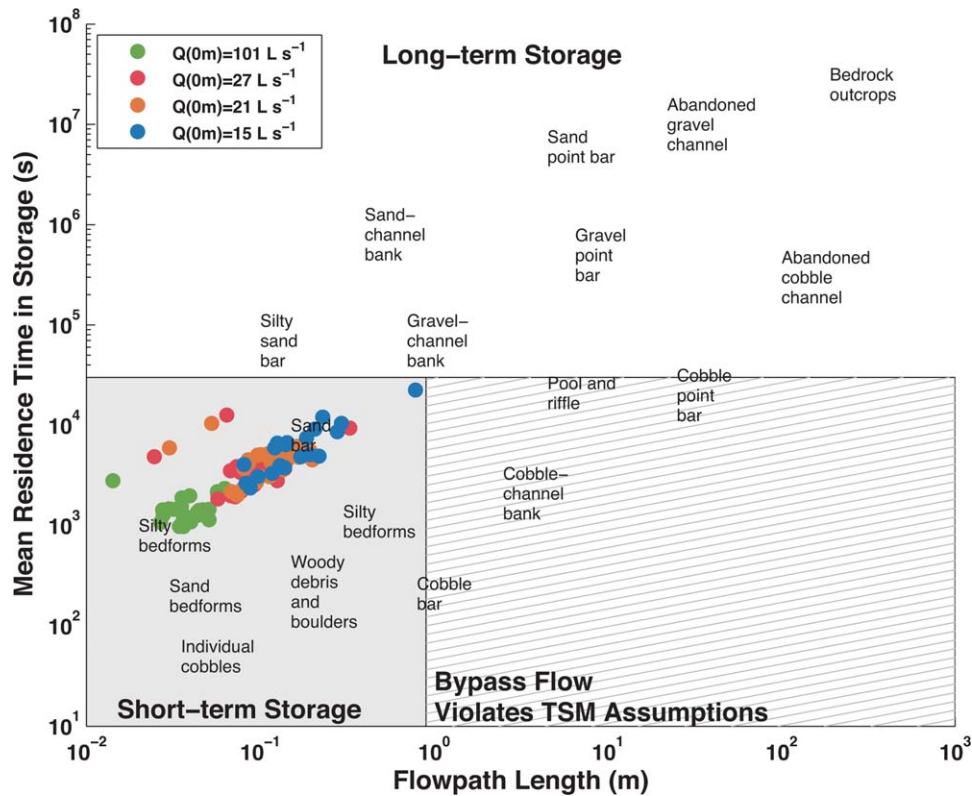


Figure 11. The maximum spatial and temporal scales of flow paths for recovered tracer are plotted relative to typical spatial and temporal scales of hyporheic exchange due to natural stream features [after Figure 11 from *Harvey and Wagner, 2000*]. The combined analysis allows the range of possible flow paths to at least be divided into those returning and not returning to the stream during the tracer study. Timescales (Y -axis) were based on the observed t_{99} for each study; spatial scales are the calculated L_c of equation (10) (using Darcy's Law assuming valley slope was equal to hydraulic gradient, hydraulic conductivity of $1.0 \times 10^{-4} \text{ m s}^{-1}$ and porosity of 0.25).

this study overwhelmed any spatial organization in storage characteristics inherent in our generally gaining study stream. As such, the ability to conduct directly comparable studies of short- and/or long-term storage at different spatial locations in a network or at a single location under different hydrologic conditions by simply maintaining a uniform methodology is not possible; changes in the window of detection confound interpretation of results and cannot be distinguished from changes in the physical system. Indeed, even the same discharge may be a poor indicator of the ability to compare injections. Consider, for example, replicate injections completed at the same discharge on the rising and falling limbs of a storm event; valley bottom hydrology may not be expected to have the same physical processes occurring under both conditions despite the same discharge. We are unable to parse the limitations of the method from our interpretation of transport processes in streams, beyond the bulk differentiation between short- and long-term storage (a division which itself is a function of the window of detection of the tracer study). One possibility to more completely characterize short- and long-term storage might be to conduct many solute injections with different windows of detection). For example, an instructive study might be executing multiple series of tracer injections over the same study reach, but at different reach-length resolutions. Comparisons of water

balance and transient storage at different resolutions in the same stream might reveal how interpretations of hydrologic storage of channel water are potentially biased by the window of detection.

[41] Many studies use spatially sparse data collected under the same hydrological conditions (i.e., within periods of several days during which no hydrologic perturbations have occurred) to extrapolate to network behavior [e.g., *Alexander et al., 2000, 2007; Briggs et al., 2010; Wollheim et al., 2006; Ensign and Doyle, 2006; Covino et al., 2011*]. *Stewart et al.* [2011] found heterogeneity in study segment could overwhelm the underlying spatial trends that were expected. Our observations of discontinuous patterns in space and with hydrologic conditions support this conclusion; we find heterogeneity within our study segment generally overwhelms any expected patterns or gradients in short- or long-term storage, though larger spatial scale gradients (e.g., contrasts between geologic settings in the upper and lower half of the network) have been documented [*Patil et al.; Payn et al., 2012*].

5. Conclusions

[42] Solute tracer studies can be used to characterize a broad suite of short- and long-term storage flow paths in the valley bottom. From the stream's perspective,

short- and long-term storage represent similar physical processes (i.e., water and solutes exiting the advection-dominated stream channel). From a valley-bottom perspective, short- and long-term storage represent different temporal (and likely different spatial) scales of stream-aquifer interaction. Short- and long-term storage are highly heterogeneous in both space (i.e., along the valley bottom) and time (i.e., during different hydrologic conditions). Discharge is a poor predictor of short- and long-term storage interpreted from solute tracer studies in our stream; further study in additional systems would be necessary to determine if this is unique to our site, or if this is a generalizable conclusion.

[43] Results of this study demonstrate that our ability to distinguish short-term (i.e., stored solute tracer that returned to stream within the study window of detection) and long-term storage (i.e., stored solute tracer that did not return to stream during experiment) is limited by the window of detection [as was found in *Harvey et al.*, 1996; *Harvey and Wagner*, 2000]. Furthermore, the window of detection in our study is spatiotemporally variable to the degree that it may overwhelm any spatial or hydrologic organization of interpreted physical processes, even for contiguous stream reaches. The coupled interpretation of short- and long-term storage from solute tracer studies does, however, contribute to understanding of flow-path behavior both within and beyond the window of detection of a tracer injection. The differentiation between the two types of flow paths is a function of tracer study design, the physical setting, and the hydrologic conditions during the study. This dependence underscores the difficulty in developing discharge-dependent relationships to characterize solute transport through coupled stream-aquifer systems. Results of this study challenge conceptual models that stream discharge is a master variable controlling fluxes of water and solutes between streams and their valleys, and suggests careful analysis of methods is required to interpret tracer study data. While it is possible that such predictable relationships exist, we conclude solute tracer studies are not a reliable way to derive such relationships from field data due to inherent limitations with their application and interpretation.

[44] In summary, we completed solute tracer studies to analyze short- and long-term storage in 28 contiguous study reaches under four base-flow conditions. We found that metrics of short- and long-term storage are not organized with a consistent pattern in space. We found that metrics of short- and long-term storage followed no consistent spatial patterns for an individual study reach under different base-flow conditions. We found that no spatial or temporal patterns of short- and long-term storage were apparent at the whole network scale across the base-flow conditions studies. These results suggest heterogeneity between study reaches may overwhelm any expected gradient. Furthermore, the variable window of detection between spatial locations and hydrologic conditions is a master variable in our interpretations of both short- and long-term storage. Changing window of detection between individual solute injections confounds interpretation of short- and long-term storage comparisons in space and time.

[45] **Acknowledgments.** We thank the personnel at the U.S. Forest Service Rocky Mountain Research Station, Tenderfoot Creek Experimen-

tal Forest for their support. This material is based upon work supported by the National Science Foundation's Hydrologic Sciences program, under grant no. EAR-0911435. Any opinions, findings, and conclusion or recommendations expressed in this document are those of the authors and do not necessarily reflect the views of the National Science Foundation, U.S. Geological Survey, or U.S. Forest Service. Our thanks to Judson Harvey, two anonymous reviewers, and the Associate Editor, all of whom provided comments that improved the quality of this manuscript and furthered our thinking on the subject.

References

- Alexander, R., R. Smith, and G. Schwarz (2000), Effect of stream channel size on the delivery of nitrogen to the Gulf of Mexico, *Nature*, 403(6771), 758–761.
- Alexander, R., E. Boyer, R. Smith, G. Schwarz, and R. Moore (2007), The role of headwater streams in downstream water quality, *J. Am. Water Resour. Assoc.*, 43(1), 41–59.
- Baxter, C., F. Hauer, and W. Woessner (2003), Measuring groundwater-stream water exchange: New techniques for installing minipiezometers and estimating hydraulic conductivity, *Trans. Am. Fish. Soc.*, 132(3), 493–502.
- Bencala, K., and R. Walters (1983), Simulation of solute transport in a mountain pool-and-riffle stream: A transient storage model, *Water Resour. Res.*, 19(3), 718–724.
- Bencala, K. E., M. N. Gooseff, and B. A. Kimball (2011), Rethinking hyporheic flow and transient storage to advance understanding of stream-catchment connections, *Water Resour. Res.*, 47, W00H03, doi:10.1029/2010WR010066.
- Briggs, M. A., M. N. Gooseff, B. J. Peterson, K. Morkeski, W. M. Wollheim, and C. S. Hopkinson (2010), Surface and hyporheic transient storage dynamics throughout a coastal stream network, *Water Resour. Res.*, 46, W06516, doi:10.1029/2009WR008222.
- Butturini, A., and F. Sabater (1999), Importance of transient storage zones for ammonium and phosphate retention in a sandy-bottom Mediterranean stream, *Freshwater Biol.*, 41(3), 593–603.
- Covino, T., B. McGlynn, and J. Mallard (2011), Stream-groundwater exchange and hydrologic turnover at the network scale, *Water Resour. Res.*, 47(12), W12521, doi:10.1029/2011WR010942.
- Day, T. J. (1977), Field procedures and evaluation of a slug dilution gauging method in mountain streams, *N. Z. J. Hydrol.*, 16(2), 113–133.
- Ensign, S. H., and M. W. Doyle (2006), Nutrient spiraling in streams and river networks, *J. Geophys. Res.*, 111(G4), G04009.
- Fabian, M. W., T. A. Endreny, A. Bottacin-Busolin, and L. K. Lautz (2011), Seasonal variation in cascade-driven hyporheic exchange, northern Honduras, *Hydrol. Process.*, 25(10), 1630–1646.
- Fischer, H. B., E. J. List, R. C. Y. Koh, J. Imberger, and N. H. Brooks (1979), *Mixing in Inland and Coastal Waters*, Academic, New York.
- Gooseff, M., and B. McGlynn (2005), A stream tracer technique employing ionic tracers and specific conductance data applied to the Maimai catchment, New Zealand, *Hydrol. Process.*, 19(13), 2491–2506.
- Gooseff, M. N., S. M. Wondzell, and K. E. Bencala (2008), Solute transport along stream and river networks, in *River Confluences, Tributaries and the Fluvial Network*, edited by S. Rice, A. Roy, and B. Rhodes, pp. 395–418, John Wiley, West Sussex, U. K.
- Gupta, A., and V. Cvetkovic (2000), Temporal moment analysis of tracer discharge in streams: Combined effect of physicochemical mass transfer and morphology, *Water Resour. Res.*, 36(10), 2985–2997.
- Hart, D. R., P. J. Mulholland, E. R. Marzolf, D. L. DeAngelis, and S. P. Hendricks (1999), Relationships between hydraulic parameters in a small stream under varying flow and seasonal conditions, *Hydrol. Process.*, 13(10), 1497–1510.
- Harvey, C., and S. Gorelick (1995), Temporal moment-generating equations: Modeling transport and mass transfer in heterogeneous aquifers, *Water Resour. Res.*, 31(8), 1895–1911.
- Harvey, J. W., and B. J. Wagner (2000), Quantifying hydrologic interactions between streams and their subsurface hyporheic zones, in *Streams and Ground Waters*, edited by J. B. Jones and P. J. Mulholland, pp. 3–44, Academic Press, San Diego, Calif.
- Harvey, J. W., B. J. Wagner, and K. E. Bencala (1996), Evaluating the reliability of the stream tracer approach to characterize stream-subsurface water exchange, *Water Resour. Res.*, 32(8), 2441–2451.
- Jencso, K., B. McGlynn, M. Gooseff, S. Wondzell, K. Bencala, and L. Marshall (2009), Hydrologic connectivity between landscapes and streams: Transferring reach-and plot-scale understanding to the catchment scale, *Water Resour. Res.*, 45(4), W04428, doi:10.1029/2008WR007225.

- Jencso, K. G., B. L. McGlynn, M. N. Gooseff, K. E. Bencala, and S. M. Wondzell (2010), Hillslope hydrologic connectivity controls riparian groundwater turnover: Implications of catchment structure for riparian buffering and stream water sources, *Water Resour. Res.*, 46(10), W10524, doi:10.1029/2009WR008818.
- Jin, H., and G. M. Ward (2005), Hydraulic characteristics of a small Coastal Plain stream of the southeastern United States: Effects of hydrology and season, *Hydrol. Process.*, 19(2), 4147–4160.
- Karwan, D. L., and J. E. Saiers (2009), Influences of seasonal flow regime on the fate and transport of fine particles and a dissolved solute in a New England stream, *Water Resour. Res.*, 45(11), W11423, doi:10.1029/2009WR008077.
- Lees, M., L. Camacho, and S. Chapra (2000), On the relationship of transient storage and aggregated dead zone models of longitudinal solute transport in streams (Paper 1999WR900265), *Water Resour. Res.*, 36(1), 213–224.
- Leopold, L. B., and T. Maddock (1953), The hydraulic geometry of stream channels and some physiographic implications. U.S. Geol. Surv. Prof. Pap. No. 252, Supt. of Docs, 57 pp., U.S. Gov. Print. Off., Washington, D. C.
- Marion, A., M. Zaramella, and A. Packman (2003), Parameter estimation of the transient storage model for stream-subsurface exchange, *J. Environ. Eng.*, 129(5), 456–463.
- Mason, S. J. K., B. L. McGlynn, and G. C. Poole (2012), Hydrologic response to channel reconfiguration on Silver Bow Creek, Montana, *J. Hydrol.*, 438–439, 125–136.
- Morrice, J. A., H. M. Valett, C. N. Dahm, and M. E. Campana (1997), Alluvial characteristics, groundwater-surface water exchange and hydrological retention in headwater streams, *Hydrol. Processes*, 11(3), 253–267.
- Patil, S., T. P. Covino, A. I. Packman, B. L. McGlynn, J. D. Drummond, R. A. Payn, and R. Schumer, Intra-stream variability in tracer breakthrough curves: Geomorphic controls on solute retention behavior. *J. Geophys. Res. Earth Surf.*, doi:10.1029/2012JF002455, in press.
- Payn, R., M. Gooseff, B. McGlynn, K. Bencala, and S. Wondzell (2009), Channel water balance and exchange with subsurface flow along a mountain headwater stream in Montana, United States, *Water Resour. Res.*, 45(11), W11427, doi:10.1029/2008WR007644.
- Payn, R., M. Gooseff, B. McGlynn, K. Bencala, and S. Wondzell (2012), Exploring changes in the spatial distribution of stream baseflow generation during a seasonal recession, *Water Resour. Res.*, 48(4), W04519, doi:10.1029/2011WR011552.
- Reynolds, M. (1995), Geology of Tenderfoot Creek Experimental Forest, Little Belt Mountains, Meagher County, Montana, in Hydrologic and Geologic Characterizations of Tenderfoot Creek Experimental Forest, Montana, Final Rep. RJVA-INT-92734, edited by P. Farnes et al., pp. 21–32, Interim. Res. Sta., For. Serv., U.S. Dep. of Agric., Bozeman, MT, U. S. A.
- Runkel, R. L. (1998), One-Dimensional Transport with Inflow and Storage (OTIS): A solute transport model for streams and rivers, *U.S. Geol. Surv. Water Resour. Invest. Rep.* 98–4018, 73 pp. [Available at <http://water.usgs.gov/software/OTIS/>].
- Runkel, R. L. (2002), A new metric for determining the importance of transient storage, *J. North Am. Benthol. Soc.*, 21(4), 529–543.
- Schmadel, N. M., B. T. Neilson, and D. K. Stevens (2010), Approaches to estimate uncertainty in longitudinal channel water balances, *J. Hydrol.*, 394(3–4), 357–369.
- Schmid, B. H. (1995), On the transient storage equations for longitudinal solute transport in open channels: Temporal moments accounting for the effects of first-order decay, *J. Hydraulic Res.*, 33(5), 595–610.
- Schmid, B. H. (2002), Persistence of skewness in longitudinal dispersion data: Can the dead zone model explain it after all? *J. Hydraul. Eng.*, 128(9), 848–854.
- Schmid, B. H. (2003), Temporal moments routing in streams and rivers with transient storage, *Adv. Water Resour.*, 26(9), 1021–1027.
- Schmid, B. H. (2008), Can longitudinal solute transport parameters be transferred to different flow rates? *J. Hydrol. Eng.*, 13(6), 505–509.
- Schmid, B. H., I. Innocenti, and U. Sanfilippo (2010), Characterizing solute transport with transient storage across a range of flow rates: The evidence of repeated tracer experiments in Austrian and Italian streams, *Adv. Water Resour.*, 33(11), 1340–1346.
- Stanford, J. A., and J. V. Ward (1993), An ecosystem perspective of alluvial rivers: Connectivity and the hyporheic corridor, *J. North Am. Benthol. Soc.*, 12(1), 48–60.
- Stewart, R. J., W. M. Wollheim, M. N. Gooseff, M. A. Briggs, J. M. Jacobs, B. J. Peterson, and C. S. Hopkins (2011), Separation of river network-scale nitrogen removal among the main channel and two transient storage compartments, *Water Resour. Res.*, 47(1), W00J10, doi:10.1029/2010WR009896.
- Stream Solute Workshop (1990), Concepts and methods for assessing solute dynamics in stream ecosystems, *J. North Am. Benthol. Soc.*, 9(2), 95–119.
- Thackston, E. L., and K. B. J. Schnelle (1970), Predicting effects of dead zones on stream mixing, *Journal of the Sanitary Engineering Division*, 96(2), 319–331.
- Vannote, R. L., G. W. Minshall, K. W. Cummins, J. R. Sedell, and C. E. Cushing (1980), The river continuum concept, *Can. J. Fish. Aquat. Sci.*, 37(1), 130–137.
- Wagner, B., and J. W. Harvey (1997), Experimental design for estimating parameters of rate-limited mass transfer: Analysis of stream tracer studies, *Water Resour. Res.*, 33(7), 1731–1741.
- Wang, L., M. B. Cardenas, W. Deng, and P. C. Bennett (2012), Theory for dynamic longitudinal dispersion in fractures and rivers with Poiseuille flow, *Geophys. Res. Lett.*, 39, L05401, doi:10.1029/2011GL050831.
- Wollheim, W. M., C. J. Vorosmarty, B. J. Peterson, S. P. Seitzinger, and C. S. Hopkins (2006), Relationship between river size and nutrient removal, *Geophys. Res. Lett.*, 33, L06410, doi:10.1029/2006GL025845.
- Wondzell, S. (2006), Effect of morphology and discharge on hyporheic exchange flows in two small streams in the Cascade Mountains of Oregon, USA, *Hydrol. Process.*, 20(2), 267–287.
- Wondzell, S. M. (2011), The role of the hyporheic zone across stream networks, *Hydrol. Process.*, 25(22), 3525–3532.
- Wondzell, S. M. (2012), Hyporheic Zones in Mountain Streams: Physical processes and ecosystem functions, in *Stream Notes*, Jan.–Apr. 2012 Issue, pp. 1–10, Rocky Mt. Res. Stn., U.S. For. Serv., Fort Collins, CO, U. S. A.
- Wondzell, S. M. and M. N. Gooseff (2013), Geomorphic controls on hyporheic exchange across scales - Watersheds to particles, in *Treatise on Geomorphology*, edited by J. Shroder and E. Wohl, Vol. 9, pp. 203–218. Academic Press, San Diego, Calif.
- Zarnetske, J. P., M. N. Gooseff, T. R. Brosten, J. H. Bradford, J. P. McNamara, and W. B. Bowden (2007), Transient storage as a function of geomorphology, discharge, and permafrost active layer conditions in Arctic tundra streams, *Water Resour. Res.*, 43(7), W07410.